Protein Engineering, Design & Selection, 2016, vol. 29 no. 3, pp. 93–103
doi: 10.1093/protein/gzv064
Advance Access Publication Date: 12 January 2016
Original Article

OXFORD

Original Article

Promiscuous tumor targeting phage proteins

Amanda L. Gross[1], James W. Gillespie[1], and Valery A. Petrenko[1,*]

[1]Department of Pathobiology, College of Veterinary Medicine, Auburn University, Auburn, AL 36849, USA

*To whom correspondence should be addressed. E-mail: petreva@auburn.edu
Edited by Assaf Friedler

Received 14 August 2015; Revised 30 November 2015; Accepted 1 December 2015

Abstract

Cancer cell-specific targeting ligands against numerous cancer cell lines have been selected previously and used as ligands for cell-specific delivery of chemotherapies and various nanomedicines. However, tumor heterogeneity is one recognized problem hampering clinical translation of targeted anti-cancer medicines. Therefore, a novel class of targeting ligands is required that recognize receptors expressed between a variety of cancer phenotypes, identified here as 'promiscuous' ligands. In this work, promiscuous phage fusion proteins were first identified by a novel selection scheme to enrich for pan-cancer cell binding abilities, as indicated by conserved structural motifs identified previously in other cancer types. Additionally, peptide sequences containing a combination of motifs were identified to modulate binding. A panel of phage fusion proteins was studied for their specificity and selectivity for lung and pancreatic cancer cells. Phage displaying the fusion peptides GSLEEVSTL or GEFDELMTM, the two predominate clones with greatest binding ability, were used to modify preformed, doxorubicin-loaded, liposomes. These modified liposomes increased cytotoxicity up to 8.1-fold in several cancer cell lines when compared with unmodified liposomal doxorubicin. Taken together, these data indicate that promiscuous phage proteins, selected against different cancer cell lines, can be used as targeting ligands for treatment of heterogeneous tumor populations.

Key words: lung cancer, multi-target selection, pancreatic cancer, phage display, targeted nanomedicines

Introduction

Due to the low efficacy in controlling tumor growth by traditional tools, novel nanotechnology strategies are being used to increase the success of treatments. Nanomedicines, which are therapeutic agents encapsulated or conjugated to nano-sized carrier ranging in size from 10 to 1000 nm, show superior activity when compared with non-encapsulated chemotherapeutics (Kawasaki and Player, 2005). This increase in therapeutic efficacy is due to the nanomedicines' ability to specifically deposit drugs within the tumor microenvironment, while concurrently decreasing side effects caused by non-specific deposition observed with non-encapsulated drugs (Nakamura *et al.*, 2015). Actively targeted nanomedicines are developed through conjugation of disease-related target-binding moieties, such as antibodies or peptides, to nano-sized particles, which then directs nanomedicines to specific disease-related receptors (Haley and Frenkel, 2008). However, due to the heterogeneity commonly observed within tumors, targeting of specific receptors that are effective in the entire tumor cell population has proven difficult. Additionally, as the tumor progresses and develops metastatic lesions in distant locations, different sets of receptors are expressed in a tissue-specific manner (Danhier *et al.*, 2010). Active targeting of nanomedicines therefore requires that identification of ligands specific to the metastatic lesions also needs to be considered. Here, we first suggest that this problem can be addressed through the use of a new class of targeting ligands, which are able to recognize common receptors expressed on various cancer cells, identified here as 'promiscuous' ligands.

Phage display has been extensively used for the generation of protein ligands that interact with surface receptors across a variety of sources (Smith and Petrenko, 1997). When compared with antibodies, filamentous phage and their isolated coat proteins maintain their target binding functionality after exposure to harsh environmental conditions, including high temperatures and low pH (Brigati and Petrenko, 2005), which makes them intriguing candidates for use as targeting ligands. As described previously, the antigen-binding

power of a phage may reside in the peptide alone or it may be an emergent property of the peptide in the context of the remaining phage body or pVIII protein scaffold (Petrenko and Smith, 2000). In this work, we follow a developing paradigm that involves the use of intact phage particles and whole phage fusion proteins as targeted scaffolds in therapeutics (Petrenko and Jayanna, 2014) and as a specific interface in analytical devices (Henry *et al.*, 2015). Phage and their isolated proteins can be produced efficiently and inexpensively in large quantities, which is advantageous in comparison to antibodies (Gillespie *et al.*, 2015). A variety of platforms derived from the protein products of phage display libraries have been developed for numerous diagnostic and therapeutic applications including: (1) generation of targeted nanoparticles for gene delivery (Mount *et al.*, 2004; Gandra *et al.*, 2013), (2) development of MRI probes (Deutscher, 2010), (3) identification of ligands for mapping neoplastic and normal vasculature (Rajotte *et al.*, 1998; Ruoslahti, 2000), (4) targeted delivery of siRNA (Bedi *et al.*, 2013), (5) development of targeted nanorods for photothermal therapy (Wang *et al.*, 2014a,b), (6) identification of ligands for a variety of cancer cell lines, including pancreatic, breast, prostate and malignant glial cells to be used for active targeting of liposomes or micelles (Samoylova *et al.*, 2003; Jayanna *et al.*, 2010a,b; Wang *et al.*, 2010a,b; Fagbohun *et al.*, 2013; Bedi *et al.*, 2014; Petrenko and Jayanna, 2014; Wang *et al.*, 2014a,b), (7) epitope mapping (Gershoni *et al.*, 2007), and (8) use in analytical devices (Petrenko, 2008; Suiqiong Li, 2011).

To identify promiscuous ligands able to interact with common receptors expressed among different cancer cells, a landscape phage display library, displaying a randomized 9-mer fusion peptide on the pVIII major coat protein of the fd-tet-type phage vector f8-6, was screened through three subsequent rounds of selection against representative non-small-cell lung cancer (NSCLC) and pancreatic adenocarcinoma (PDA) cell lines as a model of tumor heterogeneity. This library, which introduces a fusion peptide at the N-terminus of the mature pVIII protein, is termed 'landscape phage' due to the dramatic change in surface architecture resulting after the insertion of foreign sequences identically expressed on each of the 4000 peptides across the surface of the virion capsid (Petrenko *et al.*, 1996; Smith and Petrenko, 1997; Kuzmicheva *et al.*, 2009a,b).

Materials and methods

Cell culture

PANC-1 (ATCC® CRL-1469™), Calu-3 (ATCC® HTB-55™), A549 (ATCC® CCL-185™) and MIA PaCa-2 (ATCC® CRL-1420™), cell lines were purchased from American Type Culture Collection (ATCC, Manassas, VA, USA) as frozen vials. No additional cell line verification was performed. Cells were cultured in 25 cm^2 cell culture-treated flasks (Corning, Corning, NY, USA) and maintained in a humidified incubator at 37°C in 5% CO_2 as described in the technical bulletins. Detailed cell culture methods are described in Supplementary Materials and Methods.

Selection of promiscuous phage ligands

The f8/9 landscape phage display library consists of ~1.4 billion phage clones, which comprises pVIII major coat proteins fused with a randomized 9-mer foreign peptides with the common sequence: NH_2-A**XXXXXXXXX**PAKAAFDSLQASATEYIGYAWAMVVVIV-GATIGIKLFKKFTSKAS-COOH, where X indicates any random amino acids of the inserted fusion peptide (Kuzmicheva *et al.*, 2009a,b). Individual phage clones selected from the f8/9 landscape library are designated by the sequence of the foreign fusion 9-mer peptide; however, all references identify the full-length, 55-mer pVIII protein unless otherwise noted. All procedures for handling phages, including propagation, purification, titering, isolation of phage clones and isolation of phage DNA, have been described (Brigati *et al.*, 2008). *Escherichia coli* (*E. coli*) strain K91BlueKan (Kan^r Hfr C thi lacZΔ M15 lac Y::mkh lacI^Q), used for propagating and titering of phages, was kindly provided by Dr. George Smith (University of Missouri, Columbia, MO, USA).

The multibillion clone f8/9 phage library (Kuzmicheva *et al.*, 2009a,b) was used in the selection scheme similar to those previously described (Fagbohun *et al.*, 2012; Bedi *et al.*, 2014) with modifications biased to enrich the selected phage population for clones with more promiscuous binding abilities towards a heterogeneous population composed of different cancer cell lines. Three rounds of selection were performed using a portion of the parent library from the preceding round, where the first round of selection was performed on a NSCLC cell line (Calu-3) and the remaining two rounds were performed on a PDA cell line (PANC-1) as summarized in Figure 1A. A detailed selection protocol is located in Supplementary Materials and Methods.

Phage capture assay: specificity and selectivity of phage clones

Unique phage clones were studied for their specificity and selectivity towards Calu-3 and PANC-1 cells in comparison to SAE cells and serum with a phage capture assay as previously described (Fagbohun *et al.*, 2012). A detailed protocol is provided in Supplementary Materials and Methods.

Intracellular fate of phage

The rate and intracellular localization of phage binding and penetration into target cells was visualized using confocal immunofluorescence microscopy. Calu-3 and PANC-1 cells were seeded in four-well chamber slides (Lab-Tek II, Nalgene) at a density of 5×10^5 cells/well and incubated overnight in a 37°C cell culture incubator with 5% CO_2. Cells were incubated with ~10^7 virions diluted in serum-free culture medium (EMEM for Calu-3 and DMEM for PANC-1 cells) for 4 h at room temperature. An additional slide remained untreated with phage and was used as a negative control. After removal of unbound phage, cells were washed three times with 1X PBS, pH 7.2 for 5 min per wash at room temperature. Cells were fixed with 4% paraformaldehyde for 15 min at room temperature and washed as above. Cells were treated with a Wheat Germ Agglutinin (WGA)-Alexa Fluor® 555 conjugate at a 1:200 dilution in blocking buffer (1% BSA in 1X PBS, pH 7.2) for 20 min at room temperature to stain cellular membranes. Following membrane staining, cells were washed and permeabilized using 0.1% Triton X-100 in 1× PBS, pH 7.2, for 10 min at room temperature. Cells were then blocked with 1% BSA for 1 h prior to the addition of a rabbit polyclonal anti-fd IgG (Smith *et al.*, 1998) (1:500 dilution in blocking buffer) for 1 h at room temperature. Subsequently, cells were washed and incubated with a 1:500 dilution of a goat monoclonal anti-rabbit Alexa Fluor®-488 conjugated antibody (Invitrogen) for 1 h in blocking buffer and washed as above. Nuclei were labeled with a 1:200 dilution of TOPRO-3 (Invitrogen) in blocking buffer for 10 min at room temperature. Cells were washed, protected with Vecta Shield mounting medium and cover slipped prior to imaging. Cells were visualized with a C1 confocal microscope and images were captured and analyzed using NIS Elements (ver. 4.20; Nikon Instruments).

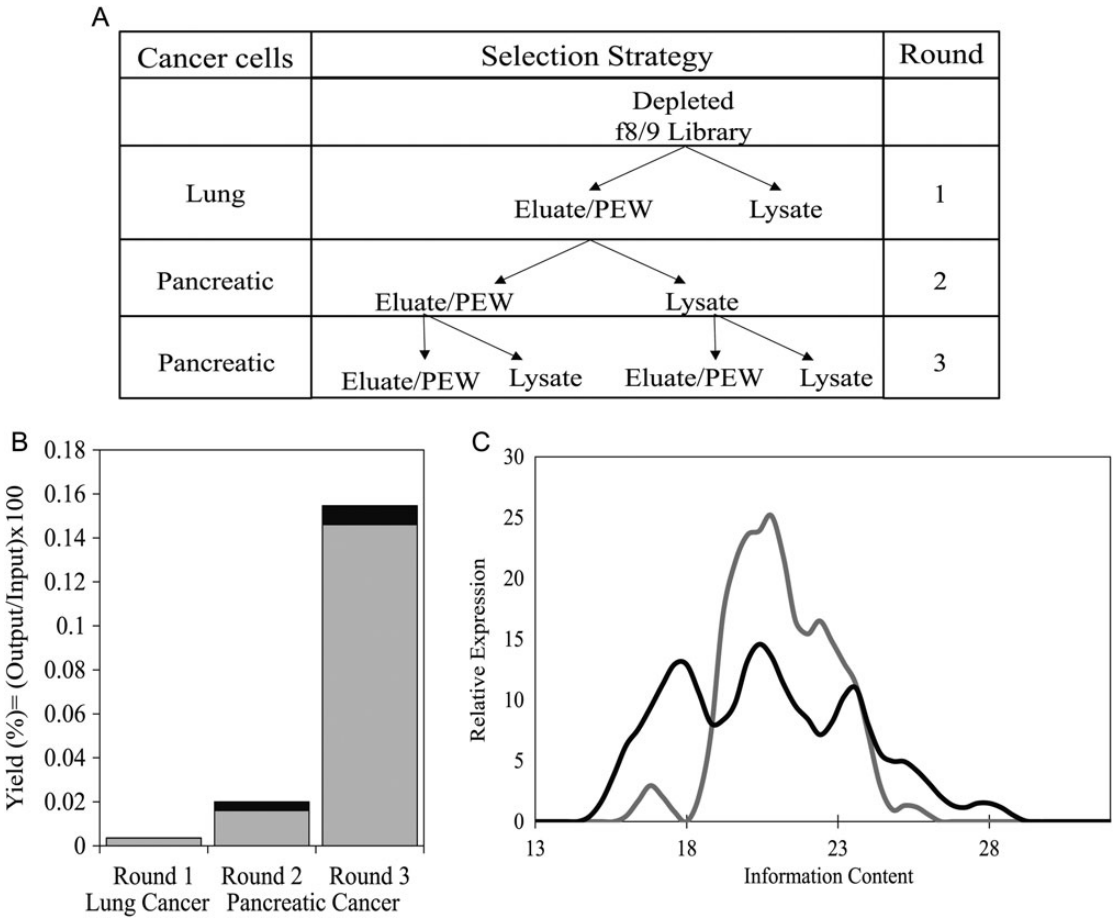

Fig. 1 Promiscuous phage display selection scheme. (**A**) Selection strategy utilizing both lung and pancreatic cancer cells to generate the eluate–eluate, eluate–lysate, lysate–eluate and lysate–lysate fractions after each round of selection. The output fractions generated from each round of selection is indicated by an arrow pointing from the input fraction. The target cells and experimental conditions for each round of selection are shown at the right. (**B**) Total phage yield after each round of selection as calculated for both the eluate (white bars) and lysate (black bars) fractions for comparison between each round of selection. (**C**) Histogram of the information content of the phage sublibrary enriched for promiscuous cancer cell-binding (black line) compared to the parent f8/9 library (gray line).

Phage major coat protein isolation

Selected phage fusion major coat proteins, pVIII, were isolated from intact phage using 2-propanol solubilization as previously described (Gillespie *et al.*, 2015) and shown in Supplementary Materials and Methods.

Preparation of phage protein-modified liposomal doxorubicin

Isolated fusion phage major coat proteins, pVIII, were mixed with Lipodox (containing 2.0 mg/ml doxorubicin) at a protein:lipid mass ratio of 1:200, immediately diluted with one volume of 1× TBS, pH 7.4 and were incubated overnight at 37°C with gentle rotation. Samples were purified using 100 K NanoSep centrifugal devices (Pall life Sciences) and washed with 1× PBS, pH 7.2, to allow for buffer exchange and removal of free doxorubicin. Purified samples were stored at 4°C until further analysis and use.

Characterization of phage protein-modified nanomedicines

Major coat protein, pVIII, incorporation into the liposomes was determined using proteinase K digestion and visualization by western blotting as previously described (Fagbohun *et al.*, 2012). Mock samples containing all components of the modified samples except protein were included as negative control samples. Changes in cell viability after treatment with phage protein-modified nanomedicines was assessed by MTT assay as previously described (Bedi *et al.*, 2014) and are discussed in Supplementary Materials and Methods. Additional physicochemical characterization assays including: size distribution, zeta potential and doxorubicin recovery are discussed in Supplementary Materials and Methods.

Results

Selection of promiscuous phage clones

The selection scheme, as outlined in Figure 1A, was performed on the f8/9 phage display library to enrich for clones with increased promiscuity towards a heterogeneous population composed of different cancer cell lines. Following recovery of phage interacting with Calu-3 cells in the first round of selection, a portion of the amplified eluate, or cell surface associated, fraction was then incubated with a PDA cell line (PANC-1) during the second and third rounds. Additionally, the temperature of phage incubation with PANC-1 cells was increased to 37°C resulting in increased active cell

transport, which allows more phage to be recovered from the lysate, or cell penetrating, fraction.

Through each successive round of selection, there was a significant increase in the total number of phage recovered in each of the eluate and lysate fractions (Fig. 1B) that can be attributed to selective enrichment of cancer cell-specific binding or cell-penetrating phage clones. Enrichment of these phages occurs through a two-stage process: (1) the removal of phage that bind plastic, serum and non-neoplastic cells and (2) through repeated rounds of incubation and amplification of recovered clones which interact with the target cells. Phage that bind cancer cell receptors with greater affinity than clones with lower affinity dominate after extensive washes and elution prior to their amplification. Remarkably, we observed an increase in overall phage yield after each subsequent round of selection even when performed using two target cell lines, PANC-1 and Calu-3. We hypothesize that the increase in phage enrichment is due to the recovery of phage clones able to interact with both populations of cancer cells.

After sequencing of *gp*VIII, analysis of the recovered clones yielded a total of 87 unique clones, representing several different families based on peptide motifs containing structurally conserved amino acids (Table I). Clones that did not reveal a shared motif were grouped into an 'orphans' family for classification. Promiscuous phage clones were compared to other selected phages that were entered into the MimoDB database (Ru *et al.*, 2010; Huang *et al.*, 2012) (version 4.3, updated July 2014) to reveal similar motifs that were identified in previous biopanning experiments with other cancer cell types and elucidate possible targets (Supplementary Table SI). One hundred and ten similar motifs were identified from the database with different targets including prostate, ovarian, bladder, skin, breast and colon cancer cells, as well as several known cancer cell markers including cancer cell-specific integrins and estrogen receptors. Several clones contained large consensus sequences, as was exemplified by the phage clone AEYGESVNA. This clone was selected previously from f8/9 phage display peptide library in a biopanning experiment that used PC-3 prostate cancer cells as their target (Jayanna *et al.*, 2010a,b). We also identified a structurally conserved VSTL family, which was selected previously in biopanning experiments using breast and prostate cancers (Arap *et al.*, 1998; Newton-Northup *et al.*, 2011) in addition to the cell lines explored in this study (Table II).

Statistical analysis of the resulting phage sublibraries was performed using the RELIC suite of programs, which was specifically developed to study combinatorial peptide libraries (Mandava *et al.*, 2004). The information content of a given phage clone is a calculated, numerical quantity that compares the probability of an amino acid from occurring randomly in the parent library to the probability that the amino acid will be present following a biopanning experiment. Thus, a phage with high information content is assumed to have a low probability of occurrence in an unselected library due to an underrepresentation of certain amino acids, but may be enriched in the population after a biopanning experiment due to specific interactions with the target or other selective pressure. It is hypothesized that following a biopanning experiment, there will be an increase in high information content phage and a decrease in low information content phage. Total information content associated with the final promiscuously selected sublibrary was determined and compared with the initial f8/9 library. Eighty-seven unique clones were analyzed as representative clones of the output sublibrary in comparison to 64 random clones that were representative of the primary f8/9 library (Fig. 1C). An increase in higher information clones was observed following sublibrary generation of promiscuous cancer cell-binding clones (black line) in comparison to the primary library (gray line) as was hypothesized. Phage clones that contained higher information content were: EVNVEEINL, EVSVEEINL, EDFAEIMQA and AEYGESVNA. All of which displayed higher binding to at least one of the target cell lines as discussed in the following section. Additionally, we see a decrease in the overall diversity of the promiscuous sublibrary following selection in comparison with a random sublibrary. These data suggest that the selected promiscuous cancer cell-binding population is enriched for phage that can bind lung and pancreatic cancer.

Specificity and selectivity of phage towards cancer cells

To determine the specificity of each clone, where specificity can be generally defined as the ability of a peptide sequence to interact with a given target, unique clones were screened using a phage capture assay against the PANC-1 cell line and culture medium containing 10% FBS (denoted as 'serum'). The resulting percent yield of each phage to each target was calculated as described in Materials and methods. To eliminate slow growing, low binding, or otherwise inefficient clones from further study, a panel of the top 20 clones was generated. These top 20 clones were identified based on the clones that demonstrated the highest recovery of phage interacting with PANC-1 cells and also demonstrated the largest ratio between PANC-1 and serum percent yields (Fig. 2A).

The top 20 clones were then screened for their selectivity, as defined as the ability of a peptide sequence to discriminate between related targets and bind to the desired target. Here, the target cells PANC-1 and Calu-3 were used in a phage capture assay to compare the interactions of phage clones with the non-target cell line, small airway epithelial (SAE) cells and unrelated components in serum. Results from selectivity screening demonstrate that clones identified following a promiscuous selection scheme show a higher selectivity to the two different types of cancer cells rather than phenotypically normal cells or serum (Fig. 2B). Based on data from both phage capture assays, two of the top clones that demonstrated selective binding to the target cells with minimal non-specific binding were GSLEEVSTL and GEFDELMTM. The GSLEEVSTL clone displayed a total recovered phage yield of 0.068% to the PANC-1 cell line and 0.056% to the Calu-3 cell line. There was a significant difference in binding observed between target cells when compared with unrelated targets ($P \leq 0.0001$ for both cell lines when compared with SAE; and $P = 0.0003$ [PANC-1] and $P = 0.0017$ [Calu-3] when compared to serum), suggesting this phage has a higher affinity to the target cells than unrelated targets. Similarly, the GEFDELMTM clone displayed a total recovered phage yield of 0.041% to the PANC-1 cell line and 0.10% to the Calu-3 cell line. Again, there was a statistically significant difference in binding observed between target cells when compared with phenotypically normal cells ($P = 0.0003$ [PANC-1] and $P < 0.0001$ [Calu-3]), suggesting that this phage has a higher affinity to the target cells than phenotypically normal cells. There was also a statistically significant difference in phage binding observed between the Calu-3 cell line and serum binding ($P < 0.0001$). However, a difference in binding was not observed for this phage when comparing binding to PANC-1 and serum ($P = 0.0385$). Additionally, when looking at phage clones that bound either cell line strongly while still having a moderate affinity for the other, the top clones include DHVWAEGDS ($P < 0.0001$ and 0.0016 for Calu-3 versus SAE and Serum, respectively) and DPNWEATVG ($P < 0.0001$ for Calu-3 and both SAE and Serum) for Calu-3 and AEYGESVNA ($P = 0.0105$ for PANC-1 and SAE) for PANC-1. Five clones (GSLEEVSTL, GEFDELMTM, DHVWAEGDS, DPNWEATVG and AEYGESVNA), which demonstrate high selectivity and specificity to

Table I. Analysis of phage clone motifs

AEV-TL	*DGR*	*DHV*	*EFD*	*EVT*	*GSL-E-STL*	*PEV*	*SVD*	*WSP---D*
ADT**AEVSTL**	**DGR**GYSSED	DGRPP**DHV**D	ESTRGL**EFD**	DPLA**EVT**TL	**GSLAETSTL**	GSD**PEV**VHL	GSA**SVD**MDM	EP**WSP**TMG**D**
DPL**AEVTTL**	**DGR**HLDQVD	**DHV**WAEGDS	G**EFD**ELMTM	EYAMR**EVT**E	**GSLEEVSTL**	VGWS**PEV**PD	VQAFDD**SVD**	VG**WSP**EVP**D**
AFD	**DGR**ADLSYD	*DYS*	*ELVS*	*FDP*	*GTG*	*PGD*	*VDG*	*YGE*
AFDPDLHLN	**DGR**AYDVNE	AFGED**DYS**D	DYNP**ELVS**L	A**FDP**DLHLN	DELILV**GTG**	AF**PGD**ESDT	DGRFG**VDG**S	AE**YGE**SVNA
VQ**AFD**DSVD	A**DGR**DHYSD	E**DYS**ELVSQ	SDYS**ELVS**Q	VT**FDP**YDNN	DGRDG**GTG**S	GWGT**PGD**VD	DGRPDT**VDG**	D**YGE**EAINV
AEI	**DGR**DGGTGS	*ED-SEL*	*EPG(MD)*	*GDE*	*GVD*	*RAD*	**VDG**RLGDEH	*YNE*
EDF**AEI**MQA	**DGR**DHSGQD	**ED**I**SEL**NTL	ATG**EPGMD**A	AFP**GDE**SDT	DGRF**GVD**GS	DG**RAD**LSYD	**VDG**RMGDMG	AT**YNE**SVNE
GNM**AEI**TSL	**DGR**FGVDGS	**ED**Y**SEL**VSQ	VAVS**EPGMD**	DGRSIV**GDE**	VDWSTD**GVD**	VGIDEQ**RAD**	*VDW*	DGRMTV**YNE**
ASV	**DGR**FSDMPT	*EEA*	VY**EPG**LGTD	DVDGRL**GDE**	*GYSSE*	*REV*	**VDW**DNVSES	*Orphans*
GS**ASV**DMDM	**DGR**MGSEVS	AVGS**EEA**LL	*ESD*	*GDD*	DGR**GYSSE**D	DNG**REV**GND	**VDW**STDGVD	AVHDQDYDS
GSFSE**ASV**S	**DGR**MTVYNE	DYG**EEA**INV	AFPGD**ESD**T	DGRMVM**GDD**	**GYSSE**HLID	EYAM**REV**TE	*VEE(INL)*	DAASHNAED
AVG	**DGR**MVMGDD	*EEG-YIAA*	DGRSVM**ESD**	VLR**GDD**MNN	*G---E-STV*	*SEE*	EVN**VEEINL**	DNPWGLQPD
AVGSEEALL	V**DGR**MGDMG	G**EEG**E**YIAA**	*EST*	*GED*	**G**GED**EESTV**	AVG**SEE**ALL	EVS**VEEINL**	DPNWEATVG
GDYTE**AVG**A	**DGR**PDTVDG	V**EEGGYIAA**	**EST**RGLEFD	AF**GED**DYSD	**G**RME**E**V**STV**	VSYLE**SEE**S	**VEE**GGYIAA	DPRVESMSG
A-G-D-YSD	**DGR**PPDHVD	*EES*	GGEDE**EST**V	G**GED**EESTV	*LAE--TL*	*SES*	*VGD*	EDARTAAMA
AD**G**R**D**H**YSD**	**DGR**RDVADD	GGED**EES**TV	*E(V/T)S(TL)*	VIYPGV**GED**	DP**LAE**VT**TL**	DHYSS**SES**	DGRSI**VGD**E	EGMNYHIDQ
AFGEDDYSD	**DGR**RGEETD	VSYLES**EES**	ADTA**EVSTL**	*GEE*	GS**LAE**TS**TL**	VDWDNV**SES**	GPY**VGD**LDS	EHGNIEGNN
A---ESVN	**DGR**SIVGDE	*(E)EVST(L)*	ASME**EVSTL**	DGRR**GEE**TD	*MEEVST*	*SME*	**VGD**AGHSME	ESWGQGIPD
AEYG**ESVN**A	**DGR**SVMESD	ADTA**EVSTL**	DGRMGS**EVS**	DY**GEE**AINV	AS**MEEVST**L	A**SME**EVSTL	*VNE*	GYGFNQDQT
ATYN**ESVN**E	**DGR**YIGDND	ASM**EEVSTL**	EYDK**ETSTL**	**GEE**GEYIAA	GR**MEEVST**V	VGDAGH**SME**	ATYNES**VNE**	GYPIGGDTT
DEL	**DGR**YQDLPD	GRM**EEVST**V	GRME**EVST**V	*GSE*	*MGD*	*SSE*	DGRAYD**VNE**	RVPGSYSID
DELILVGTG	V**DGR**LGDEH	GSL**EEVSTL**	GSLA**ETSTL**	AV**GSE**EALL	DGRMV**MGD**D	DGRGY**SSE**D	*VSE*	VTLWEPDSD
GEF**DEL**MTM	V**DGR**MGDMG			DGRM**GSE**VS	EPQSPT**MGD**	DHYS**SSE**S	VA**VSE**PGMD	
					VDGR**MGD**MG	GY**SSE**HLID	VDWDN**VSE**S	

Sequenced phage clones were analyzed for similar structural motifs/families after the third round of selection and are shown in bold. Clones without an identified family are termed ‘orphans’.

Table II. Promiscuous binding motifs identified in other biopanning experiments

Promiscuous Ligand[a]	Motif-containing peptides from other selected peptides	Target/Reference
AEYGESVNA	**AEYGES**G**NA** **AEYGESV**LI **AEYGESVNA** **AEYGE**RG**NA**	Prostate Cancer (Jayanna *et al.*, 2010a,b)
DHVWAEGDS	GPN**WAEGDS**	Prostate Cancer (Jayanna *et al.*, 2010a,b)
DYNPELVSL	NHTT**EL**G**SL**MPG	Pancreatic Cancer (Huang *et al.*, 2005)
	IKAP**NP**PS**VS**TLPPR	Prostate Cancer (Newton-Northup *et al.*, 2011)
GSLEEVSTL	YPHY**SL**PGS**STL**	Lung Cancer (Zang *et al.*, 2009)
ADTAEVSTL	IKAPNPPS**VSTL**PPR	Prostate Cancer (Newton-Northup *et al.*, 2011)
ASMEEVSTL	CTC**VSTL**SC	Breast Cancer (Arap *et al.*, 1998)

Selected promiscuous phage clones shown in Supplementary Table SI. Identified cross-selected motifs were screened for similar structural motifs between other cancer cell surface markers using the MimoDB v4.3 database. Common motifs are shown in bold. Phage clones that were studied further in this project are shown, where remaining phage clones are shown in Supplementary Table SI.

the target cells, were chosen for further analysis of their cell-specific interactions and subcellular partitioning using confocal immunofluorescence microscopy.

Intracellular fate of phage in cancer cells

Identification of phage that are transported into cell membranes within a reasonable time period and identification of the subcellular location where phage accumulate are important considerations for designing novel cancer cell-specific nanomedicines. These data are also valuable in selecting phage clones that target specific subcellular organelles, such as the nucleus or mitochondria. The intracellular fate of five of the top clones, identified in the panel above, was studied by confocal immunofluorescence microscopy. Briefly, isolated clones were incubated with each of the target cell lines (PANC-1 and Calu-3) in a chamber slide for 4 h at 37°C. After the unbound phage were removed, cells were fixed with paraformaldehyde and permeabilized with Triton X-100. Phage were labeled with an anti-fd phage IgG and visualized with an Alexa Fluor 488-conjugated secondary antibody. Similarly, subcellular compartments were visualized using the WGA-Alexa Fluor 555 membrane stain, which specifically binds *N*-acetylglucosamine and *N*-acetylneuraminic acid residues, and the TO-PRO-3 nuclear stain. An unrelated phage displaying the fusion peptide VPEGAFSSD, identified previously against streptavidin (Petrenko and Smith, 2000), was used as a negative control to identify non-specific interactions. After treatment, specific accumulation of each phage clone was observed in both target cell lines (PANC-1 and Calu-3) and compared with binding observed with the unrelated control phage. Phage bearing the fusion peptides GSLEEVSTL, GEFDELMTM and DHVWAEGDS demonstrated the greatest accumulation within the cytoplasm (Fig. 3A). These phage clones also demonstrated increased accumulated within the perinuclear space after 4 h of incubation, suggesting their potential use as ligands for intracellular drug delivery and/or molecular imaging techniques. Perinuclear penetration was observed after 4 h of incubation for phage clones displaying the fusion peptides GSLEEVSTL (Fig. 3B) or GEFDELMTM (data not shown). The unrelated control phage demonstrated no binding to either of the target cell lines under the studied conditions, suggesting that the interactions were specific and due to the presence of displayed fusion peptide (Fig. 3A). It was hypothesized that these phage clones would be ideal candidates for use as targeting ligands in tumor-targeted nanomedicines, due to the ability of these phage clones to rapidly internalize within 4 h and their increased accumulation within and around the nucleus.

Modification and characterization of preformed, doxorubicin-loaded liposomes

Cancer cell-targeted variants of Lipodox (liposomal doxorubicin, containing 2 mg/ml doxorubicin) were generated by incubation of isolated pVIII fusion coat proteins bearing the fusion peptides GSLEEVSTL and GEFDELMTM with a portion of Lipodox, as previously described (Gillespie *et al.*, 2015). Isolated phage proteins spontaneously incorporate into lipid bilayers to near completion under these conditions (~100% incorporation), due to the highly hydrophobic domain within the pVIII major coat protein (Petrenko and Jayanna, 2014). The presence of phage proteins associated with liposomes following modification and purification was confirmed using SDS–PAGE followed by detection by western blotting with a polyclonal phage antibody (rabbit anti-fd IgG) (Fig. 4). We observed minimal changes in relative surface charge or size distribution following modification with either phage protein (Table III). A 6.7 and 7.5 nm increase in population diameter was observed for GSLEEVSTL- and GEFDELMTM-modified Lipodox, respectively. A 0.4 mV increase and 1.2 mV decrease in zeta potential was observed for GSLEEVSTL- and GEFDELMTM-modified Lipodox, respectively. Minimal changes in size distribution or zeta potential were assumed to not be physiologically relevant changes in the biological system being studied. The majority of the initial doxorubicin input was retained after protein insertion (~60–85% recovery; Table III).

It was hypothesized that introduction of promiscuous cancer cell-specific phage proteins would increase the cytotoxicity of unmodified Lipodox in a number of cancer cell lines including, the target cell lines, Calu-3 and PANC-1, as well as related cancer cell lines, A549 and MIA PaCa-2, demonstrating greater intrinsic doxorubicin sensitivity. To test this hypothesis, phage protein-modified Lipodox (as prepared above) and unmodified Lipodox were incubated at various doxorubicin concentrations in these cell lines for a continuous 18-hour exposure. GSLEEVSTL-modified Lipodox, when compared to unmodified Lipodox, demonstrated: (1) decreased PANC-1 cell viability at high concentrations of doxorubicin (40 and 8 μg/ml; $P < 0.0001$ and 0.0026, respectively), (2) decreased Calu-3 cell viability at high doxorubicin concentrations (200, 40 and 8 μg/ml; $P = 0.0012$, 0.0072 and 0.0043, respectively) and (3) decreased A549 cell viability at high doxorubicin concentrations (200 and 40 μg/ml; $P = 0.0015$ and < 0.0001, respectively) (Fig. 5A). We note that the GSLEEVSTL-modified Lipodox preparation was not studied in the more drug sensitive pancreatic cancer cell line, MIA PaCa-2. In summary, GSLEEVSTL-modified Lipodox demonstrated increased cytotoxicity towards PANC-1, Calu-3 and A549 cells when compared to unmodified Lipodox at matched doxorubicin

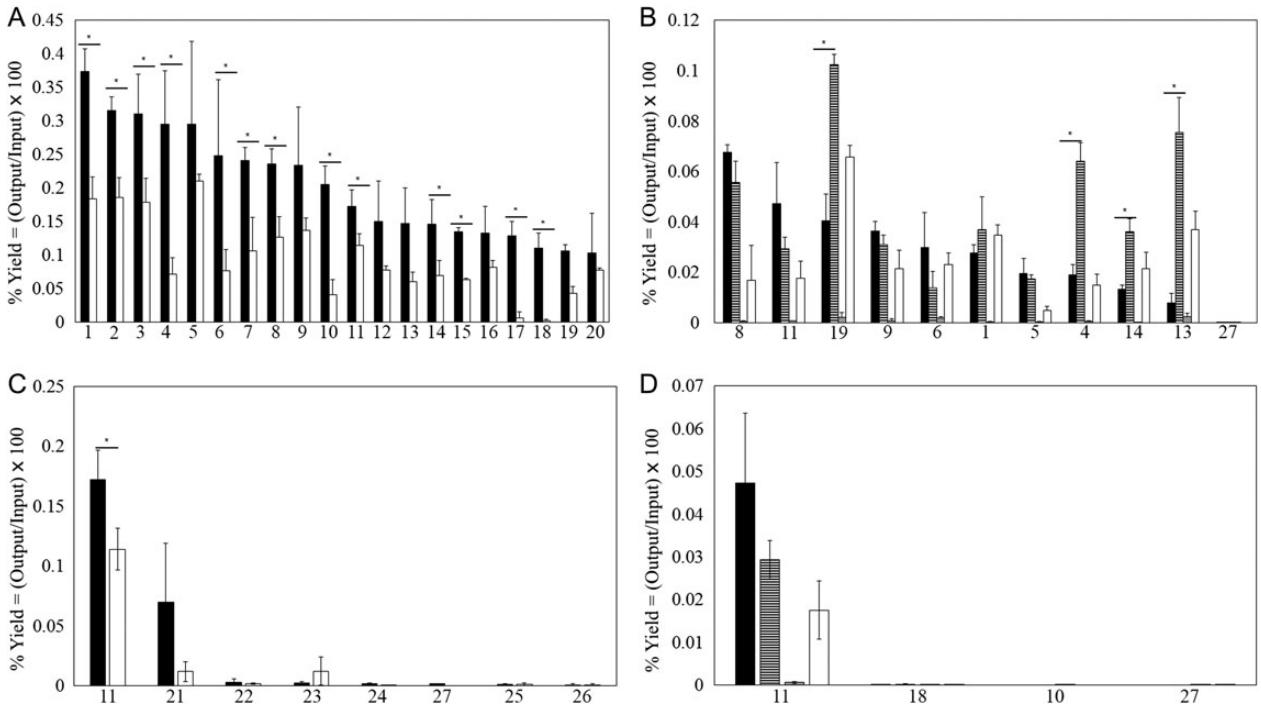

Fig. 2 Selectivity and specificity assays of phage with target cells. (**A**) Phage capture assay of representative phage clones interacting with either pancreatic cancer cells (black bars) or serum (white bars). (**B**) Phage capture assay of representative selected phage clones interacting with pancreatic cancer cells (black bars), lung cancer cells (striped bars), normal lung cells (gray bars) and serum (white bars). (**C**) Phage capture assay of representative phage clones containing a DGR and/or VDG motifs interacting with pancreatic cancer cells (black bars) or serum (white bars). (**D**) Phage capture assay comparing binding of phages containing VDG and DGR motives in pancreatic cancer cells (black bars), lung cancer cells (striped bars), normal lung cells (gray bars) and serum (white bars). For all plots, the phage clone VPEGAFSSD was included as a negative control. Data are presented as the mean percent yield ± standard deviation (SD). * indicates a *P*-value < 0.05, when comparing paired output yields. (1) EVNVEEINL; (2) EGMNYGIDQ; (3) EVSVEEINL; (4) DPNWEATVG; (5) EDARTAAMA; (6) ATYNESVNE; (7) EPWSPTMGD; (8) GSLEEVSTL; (9) GPYVGDLDS; (10) DGRADLSYD; (11) DGRPDTVDG; (12) GGEDEESTV; (13) DHVWAEGDS; (14) ADTAEVSTL; (15) DPRVESMSG; (16) DYGEEAINV; (17) DNGREVGND; (18) DGRMGSEVS; (19) GEFDELMTM; (20) AEYGESVNA; (21) DGRTIGDND; (22) DGRFSDMPT; (23) DGRDHSGQD; (24) DGRHLDQVD; (25) DGRFGVDGS; (26) VDGRMGDMG; (27) negative control.

concentrations. At the same doxorubicin concentration, 200 μg/ml, the GSLEEVSTL-modified Lipodox preparation showed a 2.4 ± 0.9-, 2.3 ± 0.1- and 8.1 ± 1.9-fold decrease in cell viability in PANC-1, Calu-3 and A549 cells, respectively, when compared with unmodified Lipodox.

Similarly, GEFDELMTM-modified Lipodox, when compared with unmodified Lipodox, demonstrated: (1) decreased PANC-1 cell viability at moderate doxorubicin concentrations (20 and 4 μg/ml; $P = 0.0003$ and < 0.0001, respectively), (2) decreased Calu-3 cell viability at both high and low concentrations of doxorubicin (100, 4 and 0.16 μg/mL; $P = 0.0068$, < 0.0001 and < 0.0001, respectively), (3) decreased A549 cell viability at high doxorubicin concentrations (100 and 20 μg/ml; $P < 0.0001$, respectively), and (4) decreased MIA PaCa-2 cell viability at high doxorubicin concentrations (100 μg/ml; $P = 0.0008$) (Fig. 5B). The GEFDELMTM-modified Lipodox preparation showed a 2.4 ± 0.1 and 2.4 ± 0.2 fold decrease in cell viability at a 100 μg/ml doxorubicin concentration in A549 and Mia-PaCa2 cells, respectively. In general, these results indicate that GSLEEVSTL-modified Lipodox and GEFDELMTM-modified Lipodox are more effective at decreasing cell viability compared to unmodified Lipodox at higher doxorubicin concentrations. These two ligands may act similarly in targeting a heterogeneous tumor population, since a decreased cell viability was demonstrated across two different cancer phenotypes (NSCLC and PDA) in a total of four cell lines (Calu-3, A549, PANC-1, and MIA PaCa-2).

Discussion

A number of cell surface receptors are aberrantly expressed in neoplastic tissues. Identification of some of these receptors was enabled through the use of phage display screening (Newton *et al.*, 2006; Sergeeva *et al.*, 2006; Jayanna *et al.*, 2010a,b; Fagbohun *et al.*, 2012; Bedi *et al.*, 2014; Guo *et al.*, 2014; Mandelin *et al.*, 2015). However, numerous screening protocols have been completed *in vitro* using a single target cancer cell line and may not accurately depict the inherent heterogeneity of tumors observed in the clinical setting. To address this issue, we hypothesized that phage ligands enriched from a combination of different cancer cell lines would demonstrate an increased binding promiscuity to multiple cancer phenotypes using a single ligand. If this hypothesis is shown to be true, there should be an increased probability of targeting ligands interacting with their receptors within a heterogeneous tumor population. It was shown previously that pVIII major coat proteins could be used as targeting ligands to modify preformed, liposomal nanomedicines (Petrenko and Jayanna, 2014). Therefore, it was hypothesized that promiscuous pVIII major coat proteins isolated through a multi-target selection strategy could increase the toxicity of existing chemotherapies in a number of different cancer cell lines with vastly different phenotypes. As a proof-of-concept, we used the previously characterized 9-mer landscape phage library, f8/9, as a source of ligands in an *in vitro* screening experiment against NSCLC and PDA cell lines as a model of tumor heterogeneity.

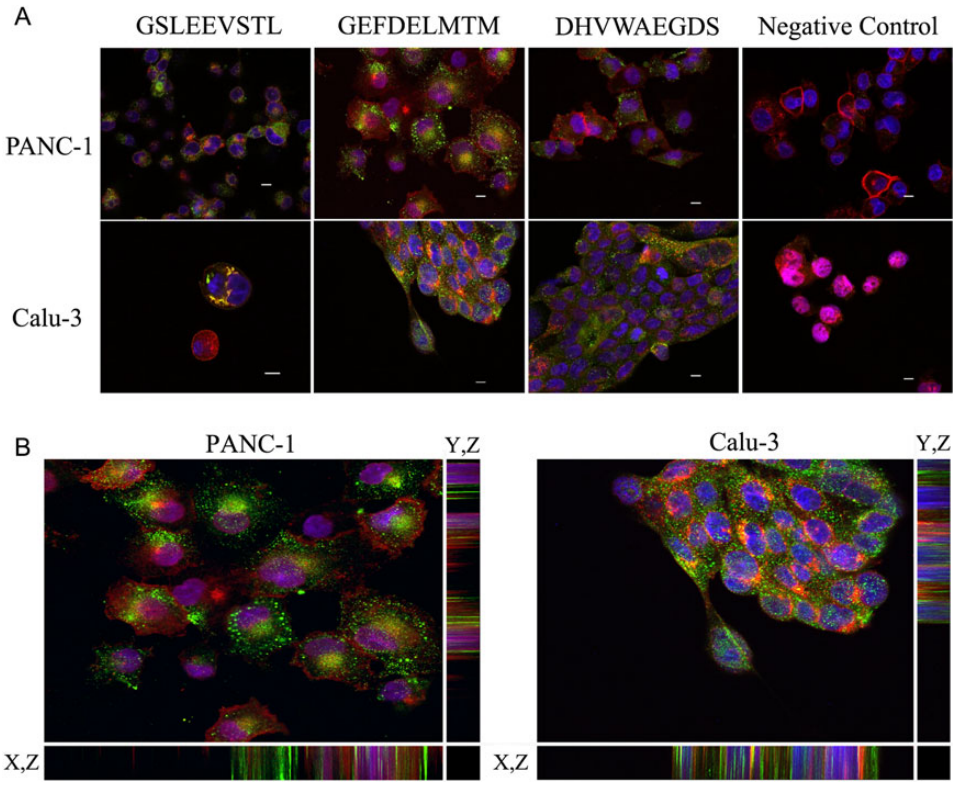

Fig. 3 Intracellular accumulation and fate of cancer cell-specific phage. (**A**) Intracellular fate of isolated phage clones in PANC-1 and Calu-3 cells. Cancer cells were incubated with 10^7 virions of each corresponding phage for 4 h and visualized using confocal immunofluorescence microscopy. Phage were visualized with an Alexa Fluor®-488-conjugated anti-fd IgG (green), membranes visualized with a WGA-Alexa Flour®-555 conjugate (red), and nuclei visualized with TO-PRO-3 (blue). All scale bars are 10 μm. (**B**) Intracellular accumulation of phage clone GSLEEVSTL. Orthogonal slices of PANC-1 or Calu-3 cells after 4 h incubation with GSLEEVSTL phage. Phage were visualized with an Alexa Fluor®-488-conjugated anti-fd IgG (green), membranes visualized with a WGA-Alexa Flour®-555 conjugate (red), and nuclei visualized with TO-PRO-3 (blue).

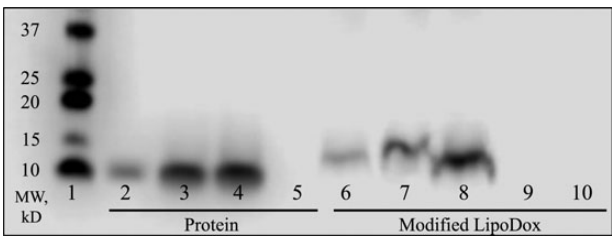

Fig. 4 Physicochemical characterization of phage protein-modified lipodox. Presence of phage protein was assayed by western blot with an anti-fd IgG after separation by SDS–PAGE. Samples: (1) 10–250 kDa marker (Bio-Rad), (2) VNGRAEAP protein, (3) EPSQSWSM protein, (4) GSLEEVSTL protein, (5) Mock sample control, (6) VNGRAEAP-modified Lipodox, (7) EPSQSWSM-modified Lipodox, (8) GSLEEVSTL-modified Lipodox, (9) Mock Lipodox sample control and (10) Unmodified Lipodox.

A number of phage clones were identified in this study as being selective for the two phenotypically different target cell lines, PANC-1 and Calu-3. Several common structural motifs were identified between phage identified in this study and those identified during other phage biopanning (screening) experiments targeting other neoplastic cells. The selection scheme presented here enables identification of ligands with different primary mechanisms of interaction with the target cells as demonstrated by our results. For example, ligands were identified that can interact with many different cell phenotypes. It is hypothesized that these types of ligands interact with a common surface receptor expressed on all target cells, which increases the apparent promiscuity by binding multiple cell types. Alternatively, ligands were also identified that contain multiple targeting motifs within the same fusion peptide and increases binding of the single ligand to multiple targets. The resulting multivalent binding allows these ligands to bind promiscuously to multiple cellular receptors that may or may not be shared between two phenotypically different cell lines.

Analysis of each of families identified in the results presented in Table I demonstrated that several clones contained more than one structurally conserved motif. It is speculated that the appearance of two distinct, functional domains within a single fusion peptide is due to the selective enrichment of certain structural motifs during the first round of selection against lung cancer cells, which persist through all additional rounds of selection. Subsequently, a secondary motif can also be enriched in additional rounds of selection against pancreatic cancer cells from the semi-randomized amino acids present in the remaining positions not occupied by the primary motif. It can be suggested that the large DGR family of phage clones identified in this biopanning experiment were enriched during the first round of selection against lung cancer cells, as was indicated by the DGR family resulting after continued selection against NSCLC cells (Gillespie *et. al.*, 2015). Primary enrichment during the first round results in the generation of a semi-randomized sublibrary with a large number of clones falling into the DGRXXXXXX family, where X can represent any amino acid. We suggest that several of the identified secondary motifs, such as GDE, GYSSE, MGD and VDG (Table IV), were the result of

Table III. Physicochemical characterization of phage protein-modified lipodox

Preparation	Size distribution (d.nm)	Zeta potential (mV)	Doxorubicin yield	
			µg	%
GSLEEVSTL-Modified Lipodox	89.2 ± 0.4	−19.5 ± 1.2	460	84.6
GEFDELMTM-Modified Lipodox	90.0 ± 1.1	−17.9 ± 0.2	340	63.4
Unmodified Lipodox	82.5 ± 0.3	−19.1 ± 0.5	540	100

Size distribution, zeta potential and doxorubicin recovery following modification of Lipodox.

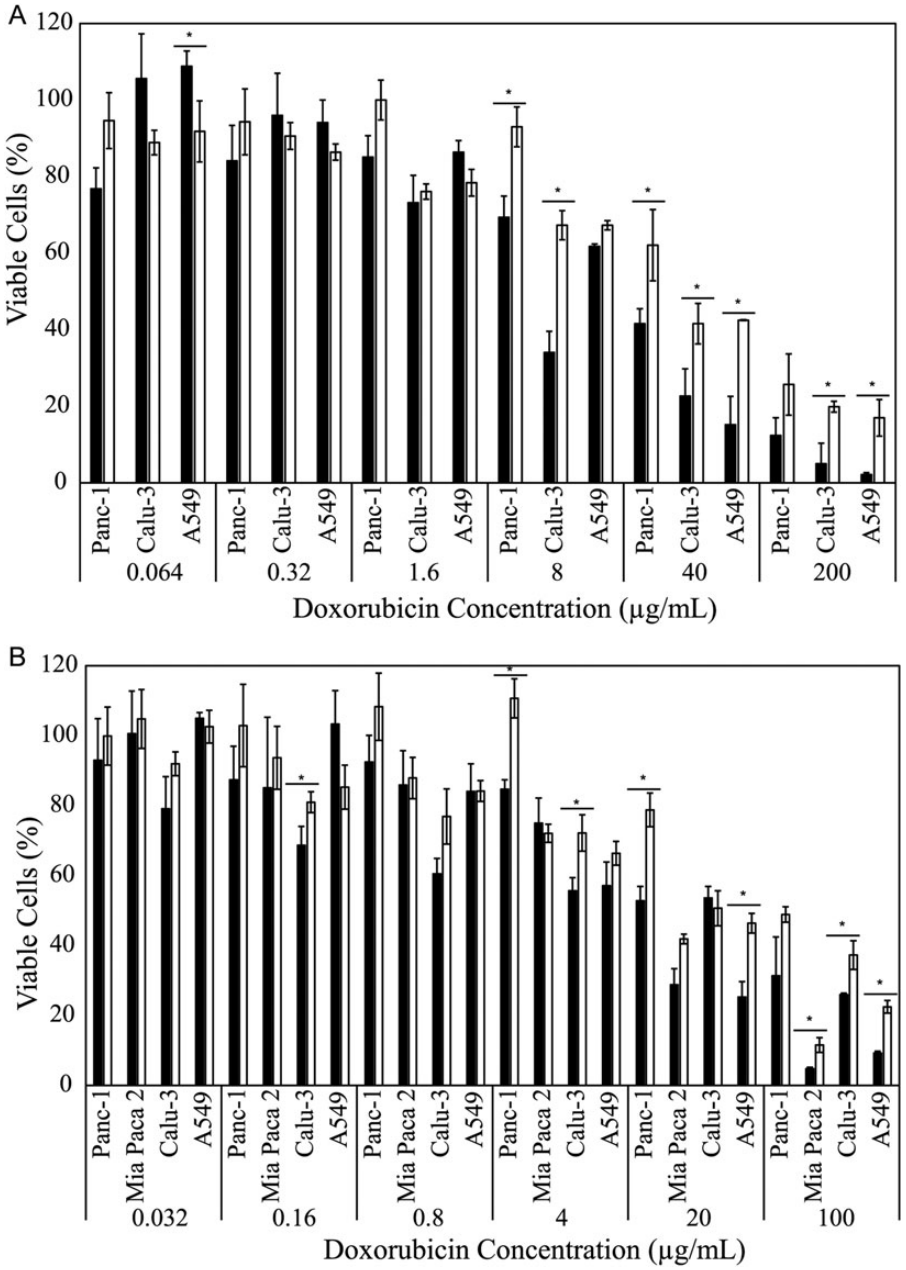

Fig. 5 Cytotoxicity of phage protein-modified lipodox. Cell viability as determined by MTT assay of GSLEEVSTL-modified Lipodox (**A**, black bars) or GEFDELMTM-modified Lipodox (**B**, black bars) compared with unmodified Lipodox (white bars) in several relevant cell lines. Percent viability was calculated by comparison of treated cells to untreated control cells, which were determined as 100% viable. * denotes a *P*-value < 0.05.

Table IV. Multivalent phage clones

1st Round of selection	2nd/3rd Round of selection
DGRXXXXXX	XXXXXX***GDE***
DGRSIVGDE	AFP***GDE***SDT
DGRFGVDGS	**DGR**SIV***GDE***
DGRGYSSED	DV**DGR**L***GDE***
DGRMVMGDD	XXX***GYSSE***X
DGRPDTVDG	**DGR*GYSSE***D
DV**DGR**LGDE	***GYSSE***HLID
V**DGR**LGDEH	XXXX***MGD***XX
V**DGR**MGDMG	**DGR**MV***MGD***D
	EPWSPT***MGD***
	V**DGR*MGD***MG
	XXXXXX***VDG***
	DGRFG***VDG***S
	DGRPDT***VDG***
	VDGRLGDEH
	VDGRMGDMG

Hypothesized enrichment scheme for selection of multivalent phage clones. During the 1st round of selection using lung cancer cells as a target, the DGR primary motif was enriched. During subsequent rounds of selection using pancreatic cancer cells as a target, secondary structurally conserved motifs were enriched.

continued enrichment of the semi-randomized DGRXXXXXX population during the second and third rounds of selection. At this time, the secondary motifs have not been independently identified during enrichment of the parent f8/9 library to PANC-1 cells. However, the presence of a secondary motif in combination with a primary motif has demonstrated significant changes in binding activity to each of the target cell lines. For example, addition of the VDG motif to a fusion peptide containing a DGR motif can significantly increase the binding of that phage clone to PANC-1 and Calu-3 cells when compared to either motif individually (Fig. 2C and D). Furthermore, the modulation in binding activity seems to be dependent on each motif acting individually. As demonstrated with the combined motif VDGR, the overall binding of the clone dramatically decreases to both cell lines (Fig. 2C). The effect of neighboring amino acids was demonstrated previously with the integrin-binding RGD motif, where the flanking amino acids impact the functionality of the peptide (Hautanen *et al.*, 1989). Here, the DGRFGVDGS clone binds minimally to PANC-1. However, enrichment of clones that replace the phenylalanine (F) residue with a proline (P) residue during selection, generating the clone DGRPDTVDG, results in significant binding to PANC-1 cell (Fig. 2C).

A combination of two types of promiscuous ligands is hypothesized to demonstrate improved intracellular delivery of actively targeted drug delivery systems and/or tumor cell-specific imaging. For example, a primary binding motif, such as the $\alpha_V\beta_5$ integrin-binding DGR motif (Koivunen *et al.*, 1993), can be responsible for identification of a specific cancer type. A secondary binding motif, such as the YSSE motif that interacts with Caveolin-1 (Couet *et al.*, 1997), may be responsible for enhancing binding or triggering a cellular response like endocytosis of the ligand. It is hypothesized that ligands can be selected that allow binding of the secondary motif to occur, only after the ligand is brought in close proximity to its receptor, as a result of interactions with the primary binding motif. Of course, it is expected that multiple, functional binding motifs may be present within the selected ligands. This hypothesis would explain the observed ability of the ligands selected in this experiment to bind various cell phenotypes derived from NSCLC and PDA tumors.

Protein ligands, identified through the promiscuous selection scheme employed here, could subsequently be used for modification of different nanomedicine platforms including liposomal or micellar scaffolds, nanorods, and generation of siRNA particles (Wang *et al.*, 2010a,b; Bedi *et al.*, 2013; Petrenko and Jayanna, 2014; Wang *et al.*, 2014a,b). Phage proteins can be used to modify preformed nanomedicines to target them specifically to a desired target or disease state and subsequently increase their activity by specific deposition of their payload within the target cells (Deutscher and Kelly, 2011). Generation of phage protein-targeted nanoparticles can be exploited not only for the delivery of chemotherapeutics, but also as tumor-specific diagnostic agents enabling earlier cancer detection and tumor-specific deposition of contrast agents or dyes that enable improved tumor evaluation and resection (te Velde *et al.*, 2010).

Numerous actively targeted nanomedicines are currently being studied in both pancreatic (Khare *et al.*, 2014) and lung cancer (Chandolu and Dass, 2013) for their efficacy in animal models and clinical trials. However, few targeted drug preparations have addressed the issue of cellular heterogeneity in primary tumors or the resulting metastatic lesions. In this study, several phage ligands were identified that selectively discriminate both pancreatic and lung cancer cell populations from phenotypically normal lung cells or serum components. These ligands display functional activity in the two cell lines against which they were selected (Calu-3 and PANC-1), as well as demonstrate functional activity in two additional cell lines from the same diseases (A549 and MIA PaCa-2). Evaluation of targeted therapies in both drug-sensitive and drug-insensitive cell lines provides an *in vitro* model system that mimics the heterogeneous drug sensitivities that are reported in clinically observed tumors (Marusyk and Polyak, 2010). Results indicate that two representative selected phage ligands increased the efficacy of liposomal doxorubicin in several cancer cell lines in comparison to unmodified liposomes, suggesting their potential applicability to treat heterogeneous cell populations with a single targeting ligand. As shown, the increase in toxicity with actively targeted nanomedicines in our study further supports the use of these ligands for targeting heterogeneous cancer cell populations. The presence of other structurally similar motifs specific for a plethora of other cancer phenotypes (Supplementary Table SI), suggest these ligands could be ideal for targeting a heterogeneous population of cancer cells.

Supplementary data

Supplementary data are available at *PEDS* online.

Acknowledgements

We would like to thank Dr. John Dennis (College of Veterinary Medicine, Auburn University) for his assistance with collection and analysis of confocal microscopy images.

Funding

This work was supported by the National Cancer Institute at the National Institutes of Health [1U54CA151881 to V.A.P] and funding support from the Auburn University Research Initiative in Cancer (AURIC) to V.A.P.

References

Arap,W., Pasqualini,R. and Ruoslahti,E. (1998) *Science*, **279**, 377–380.

Bedi,D., Gillespie,J.W., Petrenko,V.A., Jr, Ebner,A., Leitner,M., Hinterdorfer,P. and Petrenko,V.A. (2013) *Mol. Pharm.*, **10**, 551–559.

Bedi,D., Gillespie,J.W. and Petrenko,V.A. (2014) *Protein Eng. Des. Sel.*, **27**, 235–243.

Brigati,J.R. and Petrenko,V.A. (2005) *Anal. Bioanal. Chem.*, **382**, 1346–1350.

Brigati,J.R., Samoylova,T.I., Jayanna,P.K. and Petrenko,V.A. (2008) Phage display for generating peptide reagents. *Current protocols in protein science/ editorial board, John E Coligan [et al]*, **Chapter 18**, Unit 18.19. First published on 2008/04/23, doi: 10.1002/0471140864.ps1809s51.

Chandolu,V. and Dass,C.R. (2013) *Curr. Drug Discov. Technol.*, **10**, 170–176.

Couet,J., Li,S., Okamoto,T., Ikezu,T. and Lisanti,M.P. (1997) *J. Biol. Chem.*, **272**, 6525–6533.

Danhier,F., Feron,O. and Preat,V. (2010) *J. Control Release*, **148**, 135–146.

Deutscher,S.L. (2010) *Chem. Rev.*, **110**, 3196–3211.

Deutscher,S.L. and Kelly,K.A. (2011) In Petrenko,V.A. and Smith,G.P. (eds) Chap. 5 *Phage Nanobiotechnology*. London: The Royal Society of Chemistry, pp. 83–100.

Fagbohun,O.A., Bedi,D., Grabchenko,N.I., Deinnocentes,P.A., Bird,R.C. and Petrenko,V.A. (2012) *Protein Eng. Des. Sel.*, **25**, 271–283.

Fagbohun,O.A., Kazmierczak,R.A., Petrenko,V.A. and Eisenstark,A. (2013) *J. Nanobiotechnol.*, **11**, 10.

Gandra,N., Wang,D.D., Zhu,Y. and Mao,C. (2013) *Angew. Chem.*, **52**, 11278–11281.

Gershoni,J.M., Roitburd-Berman,A., Siman-Tov,D.D., Freund,N.T. and Weiss, Y. (2007) *BioDrugs*, **21**, 145–156.

Gillespie,J.W., Gross,A.L., Puzyrev,A.T., Bedi,D. and Petrenko,V.A. (2015) *Front. Microbiol.*, **6**, 628.

Guo,Y., Ma,C., Li,C., Wu,J., Zhang,D., Han,J., Wang,Q., Xu,J., Lu,S. and Hou,Y. (2014) *J. Pept. Sci.*, **20**, 196–202.

Haley,B. and Frenkel,E. (2008) *Urol. Oncol.*, **26**, 57–64.

Hautanen,A., Gailit,J., Mann,D.M. and Ruoslahti,E. (1989) *J. Biol. Chem.*, **264**, 1437–1442.

Henry,K.A., Arbabi-Ghahroudi,M. and Scott,J.K. (2015) *Front. Microbiol.*, **6**, 755.

Huang,C.H., Liu,X.Y., Rehemtulla,A. and Lawrence,T.S. (2005) *Int. J. Radiat. Oncol. Biol. Phys.*, **62**, 1497–1503.

Huang,J., Ru,B., Zhu,P., Nie,F., Yang,J., Wang,X., Dai,P., Lin,H., Guo,F.B. and Rao,N. (2012) *Nucleic Acids Res.*, **40**, D271–D277.

Jayanna,P.K., Bedi,D., Deinnocentes,P., Bird,R.C. and Petrenko,V.A. (2010a) *Protein Eng. Des. Sel.*, **23**, 423–430.

Jayanna,P.K., Bedi,D., Gillespie,J.W., DeInnocentes,P., Wang,T., Torchilin,V. P., Bird,R.C. and Petrenko,V.A. (2010b) *Nanomedicine*, **6**, 538–546.

Kawasaki,E.S. and Player,A. (2005) *Nanomedicine*, **1**, 101–109.

Khare,V., Alam,N., Saneja,A., Dubey,R.D. and Gupta,P.N. (2014) *J. Biomed. Nanotechnol.*, **10**, 3462–3482.

Koivunen,E., Gay,D.A. and Ruoslahti,E. (1993) *J. Biol. Chem.*, **268**, 20205–20210.

Kuzmicheva,G.A., Jayanna,P.K., Eroshkin,A.M., Grishina,M.A., Pereyaslavskaya,E. S., Potemkin,V.A. and Petrenko,V.A. (2009a) *Protein Eng. Des. Sel.*, **22**, 631–639.

Kuzmicheva,G.A., Jayanna,P.K., Sorokulova,I.B. and Petrenko,V.A. (2009b) *Protein Eng. Des. Sel.*, **22**, 9–18.

Mandava,S., Makowski,L., Devarapalli,S., Uzubell,J. and Rodi,D.J. (2004) *Proteomics*, **4**, 1439–1460.

Mandelin,J., Cardo-Vila,M., Driessen,W.H., *et al.* (2015) *Proc. Natl Acad. Sci. USA*, **112**, 3776–3781.

Marusyk,A. and Polyak,K. (2010) *Biochim. Biophys. Acta*, **1805**, 105–117.

Mount,J.D., Samoylova,T.I., Morrison,N.E., Cox,N.R., Baker,H.J. and Petrenko,V.A. (2004) *Gene*, **341**, 59–65. .

Nakamura,H., Jun,F. and Maeda,H. (2015) *Expert Opin Drug Deliv.*, **12**, 53–64.

Newton,J.R., Kelly,K.A., Mahmood,U., Weissleder,R. and Deutscher,S.L. (2006) *Neoplasia*, **8**, 772–780.

Newton-Northup,J.R., Figueroa,S.D. and Deutscher,S.L. (2011) *Comb. Chem. High Throughput Screen*, **14**, 9–21.

Petrenko,V.A. (2008) *Microelectronics journal*, **39**, 202–207.

Petrenko,V.A. and Jayanna,P.K. (2014) *FEBS Lett.*, **588**, 341–349.

Petrenko,V.A. and Smith,G.P. (2000) *Protein Eng.*, **13**, 589–592.

Petrenko,V.A., Smith,G.P., Gong,X. and Quinn,T. (1996) *Protein Eng.*, **9**, 797–801.

Rajotte,D., Arap,W., Hagedorn,M., Koivunen,E., Pasqualini,R. and Ruoslahti, E. (1998) *J. Clin. Invest.*, **102**, 430–437.

Ru,B., Huang,J., Dai,P., Li,S., Xia,Z., Ding,H., Lin,H., Guo,F. and Wang,X. (2010) *Molecules*, **15**, 8279–8288.

Ruoslahti,E. (2000) *Semin. Cancer Biol.*, **10**, 435–442.

Samoylova,T.I., Petrenko,V.A., Morrison,N.E., Globa,L.P., Baker,H.J. and Cox,N.R. (2003) *Mol. Cancer Ther.*, **2**, 1129–1137.

Sergeeva,A., Kolonin,M.G., Molldrem,J.J., Pasqualini,R. and Arap,W. (2006) *Adv. Drug Deliv. Rev.*, **58**, 1622–1654.

Smith,G.P. and Petrenko,V.A. (1997) *Chem. Rev.*, **97**, 391–410.

Smith,G.P., Petrenko,V.A. and Matthews,L.J. (1998) *J. Immunol. Methods*, **215**, 151–161.

Suiqiong Li,R.S.L. (2011) In Petrenko,V. and Smith,G. (eds), *Phage Nanobiotechnology*. RSC Publishing, pp. 101–156.

te Velde,E.A., Veerman,T., Subramaniam,V. and Ruers,T. (2010) *Ejso*, **36**, 6–15.

Wang,T., D'Souza,G.G., Bedi,D., Fagbohun,O., Potturi,L.P., Papahadjopoulos-Sternberg,B., Petrenko,V.A. and Torchilin,V. (2010a) *Nanomedicine (Lond)*, **5**, 563–574.

Wang,T., Petrenko,V.A. and Torchilin,V.P. (2010b) *Mol. Pharm.*, **7**, 1007–1014.

Wang,F., Liu,P., Sun,L., Li,C., Petrenko,V.A. and Liu,A. (2014a) *Sci. Reports*, **4**, 6808.

Wang,T., Hartner,W.C., Gillespie,J.W., Praveen,K.P., Yang,S., Mei,L.A., Petrenko,V.A. and Torchilin,V.P. (2014b) *Nanomedicine*, **10**, 421–430.

Zang,L.Q., Shi,L., Guo,J., Pan,Q., Wu,W., Pan,X.D. and Wang,J.Y. (2009) *Cancer Lett.*, **281**, 64–70.